

2013

Mass Transfer from a Vertical Flat Plate due to Natural Convection with a Constant Counterflow

David McDonnell

Technological University Dublin, david.mcdonnell@tudublin.ie

Brendan Redmond

Dublin Institute of Technology, brendan.redmond@tudublin.ie

Lawrence J. Crane

Institute for Numerical and Computational Analysis, lc@incaireland.org

Follow this and additional works at: <https://arrow.tudublin.ie/scschmatart>



Part of the [Mathematics Commons](#)

Recommended Citation

D. McDonnell, B. Redmond and L.J Crane, Mass Transfer from a Vertical Flat Plate due to Natural Convection with a Constant Counterflow, *Zeitschrift fuer Angewandte Mathematik und Physik (ZAMP)*, 64, 1599-1607, 2013. DOI: 10.1007/s00033-012-0298-5

This Article is brought to you for free and open access by the School of Mathematics at ARROW@TU Dublin. It has been accepted for inclusion in Articles by an authorized administrator of ARROW@TU Dublin. For more information, please contact arrow.admin@tudublin.ie, aisling.coyne@tudublin.ie.



This work is licensed under a [Creative Commons Attribution-NonCommercial-Share Alike 4.0 License](#)

Mass Transfer from a Vertical Flat Plate due to Natural Convection with a Constant Counterflow

D. McDonnell, B. Redmond and L.J. Crane

Abstract. This paper first examines the mass transfer from a vertical flat surface of a soluble material due to natural convection. A perturbation term is then introduced into the stream function to model the introduction of a constant counterflow. The effect this counterflow has on both the overall mass transfer and the overall velocity profile is studied in detail.

Mathematics Subject Classification (2010). 76R50 76R10 76M45.

Keywords. Mass Transfer, Natural Convection, Counterflow, Drug Dissolution.

1. Introduction

The aim of this paper is to first examine both the concentration and momentum boundary layers formed on a vertical flat surface due to natural convection. The surface is composed of a soluble material placed in a liquid medium. In a liquid, molecules diffuse much more slowly than momentum. Consequently, the concentration boundary layer is an order of magnitude thinner than the momentum layer. This model is analogous to that of heat transfer due to natural convection for large Prandtl numbers, for which an exact solution exists due to Kuiken[1].

The approach taken by Kuiken is to divide the problem into two regions: a thin region close to the wall in which buoyancy effects dominate and a much thicker outer region in which buoyancy effects may be neglected. In the case of mass transfer, the inner region is one of natural convection only in which the velocity is generated by the weight of dissolved particles. On obtaining a solution to this inner layer, the outer layer is treated as one of forced convection in which the velocity is generated solely by its contact with the inner layer. This case is taken as a first approximation. Having examined this first approximation, a perturbation term is introduced to the stream function to model a constant counterflow. In a reversal of the case of Kuiken, the outer layer is treated first and its solution is then matched with the inner layer. The main aim of the paper is to examine the effect that this counterflow has on the maximum downward velocity due to natural convection and consequently the effect that this has on the rate of mass transfer from the surface.

The motivation for this work comes from analysing problems in the area of drug dissolution testing. In the testing of dissolution rates from solid dosage forms it is often assumed

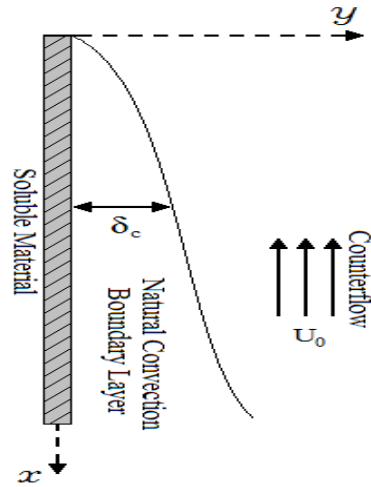


FIGURE 1. Natural Convection with a Counterflow

that the dominant mass transfer mechanism is that of forced convection, however, many of the apparatuses used in the laboratory only subject the soluble material to relatively small upward velocities. This is the case for the USP apparatus 4, known as the flow-through apparatus[2]. In such cases the role of natural convection may not be ignored. This paper takes natural convection to be the dominant mass transfer mechanism with a counterflow introduced as a perturbation term and examines the effect that this has on dissolution rates from the surface of a soluble material.

2. Mass Transfer from a Vertical Flat Plate due to Natural Convection: Kuiken

The case of heat transfer from the surface of a vertical flat plate for large Prandtl numbers was studied by Kuiken[1]. The case presented by Kuiken can be easily adapted to model mass transfer from the flat surface of a soluble material. The approach used is to split the problem into two regions: a thin inner layer in which all mass transfer takes place and buoyancy forces dominate, and an outer layer in which buoyancy forces may be neglected. The solution to the inner layer is sought first, at which point it is possible to match the outer layer to the inner solution.

The physical parameters in this problem are the kinematic viscosity(ν), the density(ρ) and the coefficient of diffusion(D). In general these quantities depend on the concentration of the solute. For example, in the case of seawater, the relative density of which is about 1.030, this dependency may not be neglected. However, in the dissolution of pharmaceutical drugs the saturation concentration is often of the order of 10^{-5} g/cm³. For example, from D'Arcy[3], the saturation concentration for Benzoic acid dissolving in water is given as 1.236×10^{-5} g/cm³. Such low concentration levels allow the values of ν , ρ and D to be taken as constant, with minimal error.

2.1. The Inner Layer

The concentration boundary layer equation is

$$u \frac{\partial c}{\partial x} + v \frac{\partial c}{\partial y} = D \frac{\partial^2 c}{\partial y^2}, \quad (2.1)$$

where x is the distance from the leading edge, y is the distance from the wall, u and v are the components of velocity in the x and y directions respectively, c is the concentration of dissolved particles and D is the coefficient of diffusion of the soluble material. The concentration layer thickness is δ_c and within this thin layer the velocity gradient is taken to be λ , where

$$\lambda = \left(\frac{\partial u}{\partial y} \right)_{y=0}.$$

Examining orders of magnitude in equation (2.1) gives

$$u \sim \lambda \delta_c, \quad v \sim u \frac{\delta_c}{x}, \quad \frac{\partial}{\partial x} \sim \frac{1}{x}, \quad \frac{\partial}{\partial y} \sim \frac{1}{\delta_c}. \quad (2.2)$$

Now, the convection terms on the left hand side of equation (2.1) must be of the same order of magnitude as the diffusion term, $D (\partial^2 c / \partial y^2)$. This gives

$$\frac{\lambda \delta_c}{x} \sim \frac{D}{\delta_c^2}, \quad (2.3)$$

which leads to

$$\frac{\lambda \delta_c^3}{x} \sim D. \quad (2.4)$$

The Boussinesq approximation is used to derive the boundary layer momentum equation, namely:

$$u \frac{\partial u}{\partial x} + v \frac{\partial u}{\partial y} = \nu \frac{\partial^2 u}{\partial y^2} + \frac{gc}{\rho}, \quad (2.5)$$

in which the effect of low concentration on the kinematic viscosity may be neglected, but must be taken into account in the last term, this being the sole driving force for the motion. In the above

equation g is acceleration due to gravity, ν is the kinematic viscosity of the dissolution medium and ρ is the density of the pure solvent. Performing a similar order of magnitude analysis as before gives

$$u \frac{\partial u}{\partial x} \sim v \frac{\partial u}{\partial y} \sim \frac{\lambda^2 \delta_c^2}{x}$$

and

$$\nu \frac{\partial^2 u}{\partial y^2} \sim \frac{\nu \lambda}{\delta_c}.$$

This leads to

$$\frac{u \frac{\partial u}{\partial x}}{\nu \frac{\partial^2 u}{\partial y^2}} \sim \frac{\lambda \delta_c^3}{\nu x}. \quad (2.6)$$

Now, from equation (2.4) we have $\lambda \delta_c^3 / x \sim D$, which gives

$$\frac{u \frac{\partial u}{\partial x}}{\nu \frac{\partial^2 u}{\partial y^2}} \sim \frac{D}{\nu} = \frac{1}{Sc}, \quad (2.7)$$

where Sc is the Schmidt number. Now for liquids, $Sc \gg 1$, and therefore the inertia terms in equation (2.5) may be neglected with error of order $1/Sc$ inside the concentration layer where the momentum boundary layer equation (2.5) reduces to

$$\nu \frac{\partial^2 u}{\partial y^2} = -\frac{gc}{\rho}. \quad (2.8)$$

Therefore, the boundary layer equations are:

$$\frac{\partial^2 u}{\partial y^2} + \frac{gc}{\rho\nu} = 0 \quad (2.9)$$

$$u \frac{\partial c}{\partial x} + v \frac{\partial c}{\partial y} = D \frac{\partial^2 c}{\partial y^2} \quad (2.10)$$

$$\frac{\partial}{\partial x}(\rho u) + \frac{\partial}{\partial y}(\rho v) = 0. \quad (2.11)$$

For very dilute solutions, ρ may be taken as constant and the continuity equation (2.11) reduces to :

$$\frac{\partial u}{\partial x} + \frac{\partial v}{\partial y} = 0. \quad (2.12)$$

Introducing $c = C_s C$, where C_s is the saturation concentration, and letting $\gamma = gC_s/\rho\nu$, equations (2.9) and (2.10) can be written:

$$\frac{\partial^2 u}{\partial y^2} + \gamma C = 0 \quad (2.13)$$

$$u \frac{\partial C}{\partial x} + v \frac{\partial C}{\partial y} = D \frac{\partial^2 C}{\partial y^2}. \quad (2.14)$$

Introducing a stream function of the form $u = \partial\psi/\partial y$, where $\psi_{\text{inner}} = kx^{\frac{3}{4}}f_0(\eta)$, $\eta = jyx^{-\frac{1}{4}}$, $j = [gC_s/4D\rho\nu]^{\frac{1}{4}}$, $k = 4D[gC_s/4D\rho\nu]^{\frac{1}{4}}$ and letting $C = h_0(\eta)$, from the continuity equation we obtain $v = -\partial\psi/\partial x$. Substituting these into equations (2.13) and (2.14), along with the required derivatives leads to the following set of ordinary differential equations:

$$f_0'''(\eta) + h_0(\eta) = 0 \quad (2.15)$$

$$h_0''(\eta) + 3f_0(\eta)h_0'(\eta) = 0. \quad (2.16)$$

Equations (2.15) and (2.16) were solved by Kuiken[1] for the following boundary conditions: at $\eta = 0$, $h_0(0) = 1$, $f_0(0) = f'_0(0) = 0$ and as $\eta \rightarrow \infty$, $h_0(\infty) \rightarrow 0$. The results obtained by Kuiken[1] are:

$$\begin{aligned} f''_0(0) &\approx 0.825 \\ h'_0(0) &\approx -0.711 \\ f'_0(\infty) &\approx 0.511. \end{aligned}$$

The resulting flux per unit area is given by:

$$\begin{aligned} \text{Flux / Unit Area} &= -D \left[\frac{\partial c}{\partial y} \right]_{y=0} \\ &= -DC_s [jh'_0(0)x^{-\frac{1}{4}}]. \end{aligned} \quad (2.17)$$

From equation (2.17), the flux per unit width is given by:

$$\begin{aligned} \text{Flux / Unit Width} &= -DC_s [jh'_0(0)] \int_0^x x^{-\frac{1}{4}} dx \\ &= -\frac{4}{3} h'_0(0) DC_s \left[\frac{gC_s}{4D\rho\nu} \right]^{\frac{1}{4}} x^{\frac{3}{4}}. \end{aligned} \quad (2.18)$$

2.2. The Outer Layer

Since there is no dissolved substance in the outer layer, the boundary layer equations are:

$$u \frac{\partial u}{\partial x} + v \frac{\partial u}{\partial y} = \nu \frac{\partial^2 u}{\partial y^2} \quad (2.19)$$

$$\frac{\partial u}{\partial x} + \frac{\partial v}{\partial y} = 0. \quad (2.20)$$

Introducing a stream function of the form $\psi_{\text{outer}} = \alpha x^{\frac{3}{4}} F(\xi)$ where $\xi = \beta y x^{-\frac{1}{4}}$, $\alpha = 4D [Sc^2/4]^{\frac{1}{4}} [gC_s/4D\rho\nu]^{\frac{1}{4}}$, $\beta = [1/4Sc^2]^{\frac{1}{4}} [gC_s/4D\rho\nu]^{\frac{1}{4}}$ and $Sc = \nu/D$, leads to the following ordinary differential equation:

$$F_0'''(\xi) + 3F_0''(\xi)F_0(\xi) - 2F_0'(\xi)F_0'(\xi) = 0. \quad (2.21)$$

In order to match the solution with that of the inner layer, equation (2.21) was solved for the following boundary conditions: at $\xi = 0$, $F_0(0) = 0$, $F'_0(0) = f'_0(\infty) = 0.511$ and as $\xi \rightarrow \infty$, $F_0(\infty) \rightarrow \text{constant}$, $F'_0(\infty) \rightarrow 0$, $F''_0(\infty) \rightarrow 0$. The results obtained are

$$\begin{aligned} F''_0(0) &\approx -0.5628 \\ f_0(\infty) &\approx 0.43. \end{aligned}$$

2.3. Velocity and Concentration Profiles

In order to plot an overall velocity profile it should be noted that $\eta = Sc^{\frac{1}{2}}\xi$. Figure 2 shows the velocity profile for both the inner and outer layer for $Sc = 100$. Figure 3 shows the concentration profile that exists within the inner layer.

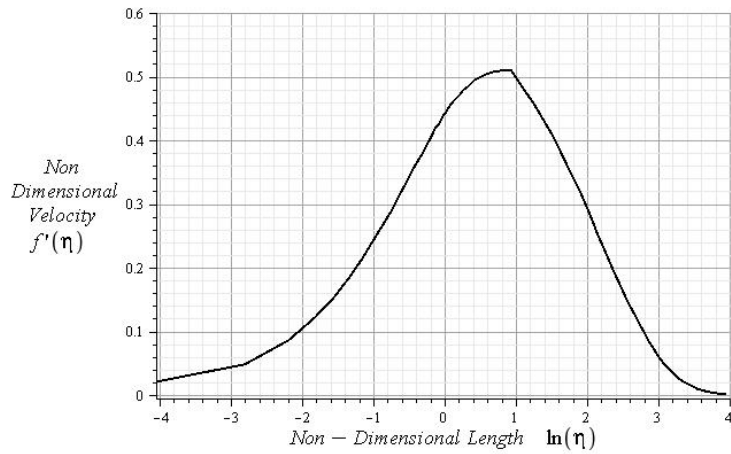


FIGURE 2. Velocity Profile: Pure Natural Convection ($Sc = 100$)

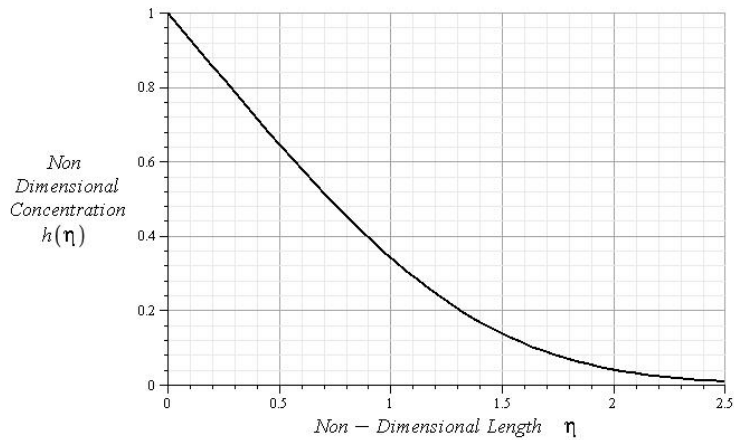


FIGURE 3. Concentration Profile: Pure Natural Convection

3. Mass Transfer for Natural Convection with a Constant Counterflow

In this section a perturbation term is introduced to the stream function in order to model a constant counterflow. The outer layer is treated first and then matched to the inner layer. The boundary layer equations for both layers are solved simultaneously by means of a shooting method. The velocity and concentration profiles are plotted for $Sc = 100$ and compared with those for the case of natural convection only. Finally an expression for the non-dimensional flux from the surface is derived.

3.1. The Outer Layer

From the outer layer solution of Kuiken[1] the stream function is given by

$$\psi_{\text{outer}} = \alpha x^{\frac{3}{4}} F_0(\xi). \quad (3.1)$$

A perturbation term is now introduced to account for a constant counterflow to give

$$\psi_{\text{outer}} = \alpha x^{\frac{3}{4}} [F_0(\xi) - \epsilon x^n F_1(\xi)], \quad (3.2)$$

where $\xi = \beta y x^{-\frac{1}{4}}$. Equation (3.2) is differentiated to give

$$u = \frac{\partial \psi}{\partial y} = \alpha \beta x^{\frac{1}{2}} F_0'(\xi) - \epsilon \alpha \beta x^{\frac{1}{2}+n} F_1'(\xi). \quad (3.3)$$

On examination of equation (3.3) it is noted that $n = -1/2$, as the upward velocity is constant and can therefore have no dependency on x . Also, at large values of ξ , the perturbation term must approach U_0 , where U_0 represents the velocity of the counterflow. This gives

$$\frac{\partial \psi}{\partial y} = \alpha \beta x^{\frac{1}{2}} F_0'(\xi) - U_0 F_1'(\xi), \quad (3.4)$$

which in turn leads to

$$\psi_{\text{outer}} = \alpha x^{\frac{3}{4}} F_0(\xi) - \frac{U_0 x^{\frac{1}{4}}}{\beta} F_1'(\xi). \quad (3.5)$$

from which the perturbation parameter is $\epsilon = U_0 x^{-\frac{1}{2}}/\alpha\beta$. This may also be written as $\epsilon = F_r [\rho S c / C_s]^{-\frac{1}{2}}$, where F_r is the non-dimensional Froude number, given as $F_r = U_0/\sqrt{g x}$. The boundary layer equations for the outer layer are

$$u \frac{\partial u}{\partial x} + v \frac{\partial u}{\partial y} = \nu \frac{\partial^2 u}{\partial y^2} \quad (3.6)$$

$$\frac{\partial u}{\partial x} + \frac{\partial v}{\partial y} = 0. \quad (3.7)$$

Introducing equation (3.5), along with the relevant derivatives, the following differential equation is obtained for the first perturbation:

$$F_1'''(\xi) + 3F_1''(\xi)F_0(\xi) - 2F_1'(\xi)F_0'(\xi) + F_1(\xi)F_0''(\xi) = 0. \quad (3.8)$$

3.2. The Inner Layer

In order to match the outer and inner layer solutions, the stream function for the inner layer is taken to be

$$\psi_{\text{inner}} = k x^{\frac{3}{4}} f_0(\eta) - \frac{U_0 x^{\frac{1}{4}}}{j} f_1(\eta), \quad (3.9)$$

where $\eta = j y x^{-\frac{1}{4}}$ and the perturbation parameter is given as $\epsilon = U_0 x^{-\frac{1}{2}}/jk$. A similar perturbation is applied to the concentration profile to yield

$$C = h_0(\eta) - \epsilon h_1(\eta). \quad (3.10)$$

The boundary layer equations for the inner layer are

$$\frac{\partial^2 u}{\partial y^2} + \frac{g C C_s}{\rho \nu} = 0 \quad (3.11)$$

$$u \frac{\partial C}{\partial x} + v \frac{\partial C}{\partial y} = D \frac{\partial^2 C}{\partial y^2} \quad (3.12)$$

$$\frac{\partial u}{\partial x} + \frac{\partial v}{\partial y} = 0. \quad (3.13)$$

Substituting equations (3.9) and (3.10), along with the relevant derivatives, into the boundary layer equations leads to the following differential equations for the first perturbation:

$$f_1'''(\eta) + h_1(\eta) = 0 \quad (3.14)$$

$$h_1''(\eta) + 2f_0'(\eta)h_1(\eta) + 3f_0(\eta)h_1'(\eta) + f_1(\eta)h_0'(\eta) = 0. \quad (3.15)$$

3.3. Velocity and Concentration Profiles

Equations (3.8),(3.14) and (3.15) where solved simultaneously using a shooting method for the boundary conditions:

$$\begin{array}{llllll} \eta = 0: & f_1(0) = 0 & f_1'(0) = 0 & f_1''(0) = \text{constant} & h_1(0) = \text{constant} & h_1'(0) = \text{constant} \\ \eta \rightarrow \infty: & f_1(\infty) \rightarrow \infty & f_1'(\infty) = F_1(0) & f_1''(\infty) = 0 & h_1(\infty) = 0 & h_1'(\infty) \rightarrow \text{constant} \\ \xi = 0: & F_1(0) = 0 & F_1'(0) = f_1'(\infty) & F_1''(0) = 0 & & \\ \xi \rightarrow \infty: & F_1(\infty) \rightarrow \infty & F_1'(\infty) = 1 & F_1''(\infty) = 0 & & \end{array}$$

The boundary condition $F_1'(0) = f_1'(\infty)$ is of particular importance, as it is the condition that matches the outer layer and inner layer solutions. The results obtained are:

$$\begin{array}{ll} F_1'(0) & \approx 0.388 \\ f_1''(0) & \approx 0.62 \\ h_1'(0) & \approx -0.36 \\ h_1(0) & \approx 0.692. \end{array}$$

The non-dimensional velocity for the inner and outer layers are:

$$\begin{aligned} f'(\eta) &= f_0'(\eta) - \frac{U_0 x^{-\frac{1}{2}}}{jk} f_1'(\eta) \\ F'(\xi) &= F_0'(\xi) - \frac{U_0 x^{-\frac{1}{2}}}{\alpha\beta} F_1'(\xi). \end{aligned}$$

Taking U_0 to be equal to 10% of the maximum downward velocity due to natural convection, which is

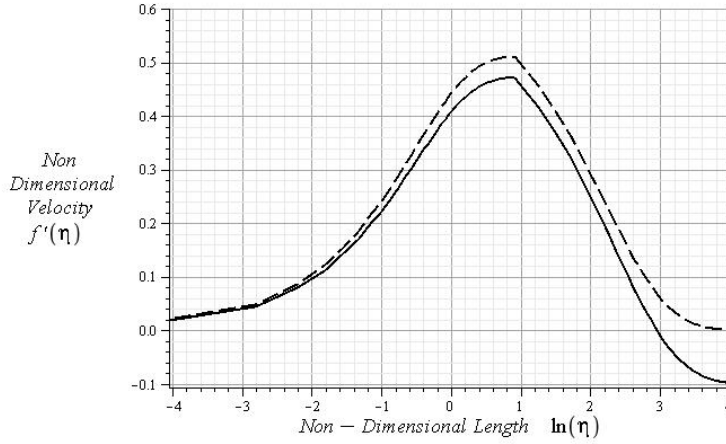


FIGURE 4. Velocity Profile: Pure Natural Convection (dashed) and Natural Convection with Counterflow (solid) for $Sc = 100$.

found to be $U_{max} = [gC_s x / \rho Sc]^{\frac{1}{2}}$, and taking $Sc = 100$, figure 4 compares the velocity profile obtained due to the counterflow with that of the solution of Kuiken. Similarly figure 5 shows the concentration profiles for both the case of pure natural convection and that of natural convection with counterflow.

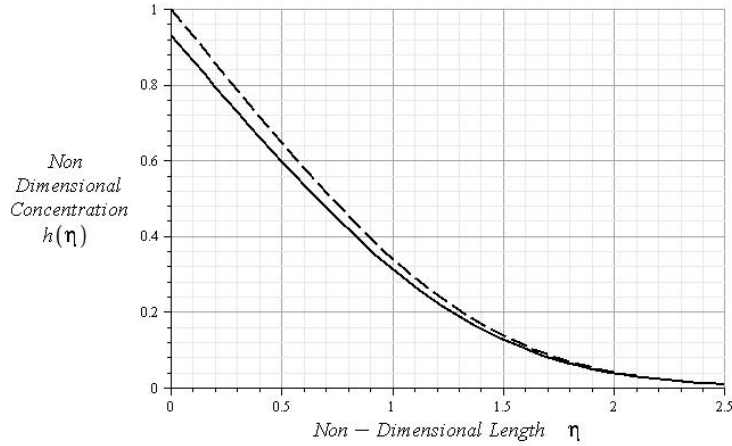


FIGURE 5. Concentration Profile: Pure Natural Convection (dashed) and Natural Convection with Counterflow (solid) for $Sc = 100$.

3.4. Flux from Surface

The flux per unit area is given by:

$$\begin{aligned} \text{Flux / Unit Area} &= -D \left[\frac{\partial c}{\partial y} \right]_{y=0} \\ &= -DC_s \left[jx^{-\frac{1}{4}} h'_0(0) - \frac{U_0}{k} x^{-\frac{3}{4}} h'_1(0) \right]. \end{aligned} \quad (3.16)$$

Integrating equation (3.16) with respect to x , the flux per unit width is found to be:

$$\text{Flux / Unit Width} = -DC_s \left[\frac{4}{3} jx^{\frac{3}{4}} h'_0(0) - \frac{4U_0}{k} x^{\frac{1}{4}} h'_1(0) \right]. \quad (3.17)$$

Equation (3.17) is divided across by the flux due to natural convection to obtain the non-dimensional flux from the surface, \tilde{M} . This is given as

$$\tilde{M} = 1 - 0.76 \left[\frac{U_0}{\sqrt{gx}} \right] \left[\frac{\rho Sc}{C_s} \right]^{\frac{1}{2}}. \quad (3.18)$$

4. Discussion

This work arose from problems in the pharmaceutical industry; more specifically in the area of drug dissolution testing of solid dosage forms. In the testing of dissolution rates the soluble material is often subject to a small vertical flow. In such cases the role of natural convection may not be overlooked. Indeed this work has taken natural convection to be the dominant mass transfer mechanism with the counterflow introduced as a perturbation term. Figure 4 shows that the outer vertical flow penetrates the inner layer leading to a significant decrease in the maximum downward velocity due to buoyancy effects. This deceleration of the inner layer flow may only be attributed to a decrease in mass transfer from the surface. Figure 5 shows the effect that the counterflow has on the overall concentration of dissolved material. Also, from equation (3.18) it can be shown that a counterflow velocity equivalent

to 10% of the maximum downward velocity due to natural convection leads to a 7.6% decrease in the mass transfer rate from the surface of the soluble material.

References

- [1] H.M. Kuiken, *An asymptotic solution for large Prandtl number free convection* Journal of Engineering Mathematics **2** (1968), 355.
- [2] United States Pharmacopeia 32, United States Pharmacopeial Convention, Rockwell, MD, USA, 2009.
- [3] D.M. D'Arcy, B. Liu, G. Bradley, A.M. Healy and O.I. Corrigan *Hydrodynamic and Species Transfer Simulations in the USP 4 Dissolution Apparatus: Considerations for Dissolution in a Low Velocity Pulsing Flow* Pharmaceutical Research **27** (2010), 246–258.
- [4] I.G. Currie, *Fundamental Mechanics of Fluids* 3rd Edition, CRC Press, 2003.
- [5] H. Schlichting, *Boundary Layer Theory* 7th Edition, McGraw-Hill, 1979.

D. McDonnell
School of Mathematical Sciences
Dublin Institute of Technology
Kevin St.
Dublin 8
Ireland
e-mail: david.mcdonnell@dit.ie

B. Redmond
School of Mathematical Sciences
Dublin Institute of Technology
Kevin St.
Dublin 8
Ireland
e-mail: B.Redmond@dit.ie

L.J. Crane
Institute for Numerical and Computational Analysis
7-9 Dame Court
Dublin 2
Ireland
e-mail: lc@incaireland.org